ICSV13 - Vienna
The Thirteenth International Congress on Sound and Vibration
Vienna, Austria, July 2-6, 2006

ABSOLUTE INSTABILITY COMPUTATIONS FOR THE PREDICTION OF TONAL SLAT NOISE

Florian Longueteau*[1], Jean-Philippe Brazier[1]

[1]Office National d'Études et de Recherches Aérospatiales
BP 4025 - 2, avenue Édouard Belin
31055 Toulouse Cedex 4, France
Florian.Longueteau@onecert.fr

Abstract

The noise generated by slats can contribute significantly to the airframe noise of an aircraft. The tonal noise in the high frequencies (4-5 kHz) of the acoustic spectrum is related to the vortex shedding in the near wake of the slat truncated trailing edge. A quantitative value of the frequency of this phenomenon is computed with linear stability tools. The influence of the main part of the wing on the eigenmodes is also examined.

INTRODUCTION

Aerodynamical and slat noise

Noise from high-lift devices, such as flaps and slats, can contribute significantly to the overall aircraft noise, particularly during the approach before landing. Consequently, many noise reduction programs have been conducted in Europe and USA during the last ten years. The review of Khorrami *et. al.* [1] shows that the acoustic spectrum of the sound radiated by the slats of a large aircraft exhibits two features for an angle of incidence of 30 degrees : a broadband component in the low to mid-frequency band (0-500 Hz), and a tonal one in the high frequencies (around 4-5 kHz). RANS/LES computations from ONERA (S. Ben Khelil *et al.* [2]), URANS computations from the NASA (M.R. Khorrami *et al.* [3]) and experiments from DLR (W. Dobrzynski *et al.* [4]) show that the flow around the slat exhibits a large scale unsteady vortex in the slat cove and a vortex shedding in the wake downstream of the slat trailing edge. It has been found that the broadband noise is related to the slat cove vortex and tonal noise to the vortex shedding (see figure 1, these computations and experiments are made on a 1/10th scale slat), which will be the subject of this study.

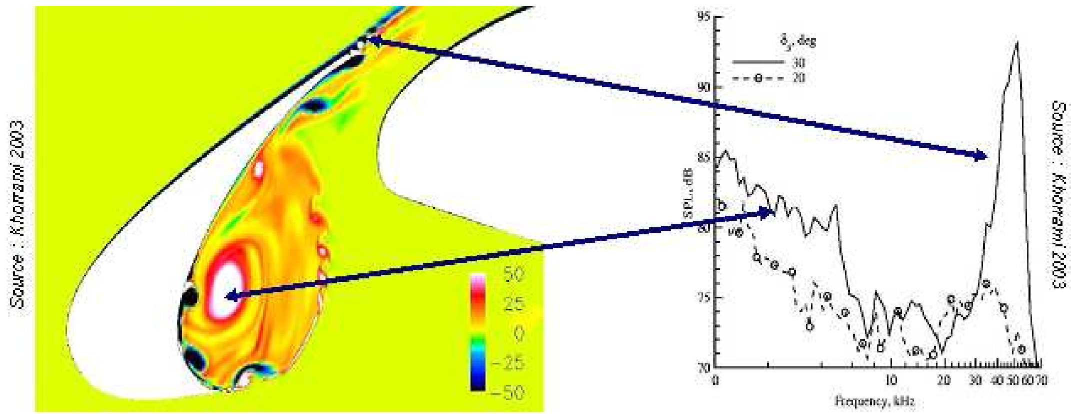

Figure 1: Relation between slat flow and his spectrum

The flow in the wake of the slat truncated trailing edge is roughly parallel and as a consequence of the continuity equation slowly varying in the streamwise direction. Just behind the edge, the flow separates in a recirculation bubble with a small counterflow which induces a zone of absolute instability. The linear stability theory seems to be one of the best ways to study this wake.

Linear stability tools

While LES computations are able to give a global resolution, a stability analysis can give, at small computing costs, an original insight concerning the mechanisms underlying the physics of the flow, and a validation of LES post-treatments. The linear stability theory of Bers [5] or Huerre and Rossi [6] for parallel flows enables to predict the vortex shedding frequency and to perform a modal study.

PROBLEM FORMULATION

Stability problem

We consider Cartesian coordinates (x, y) where x is the streamwise direction and y the crosstream one (see figure 3). The flow is assumed uniform in the spanwise direction z. In the classical stability approach, the flow variables are split into a mean part and a small perturbation (with $\varepsilon \ll 1$) :

$$\begin{cases} u(x,y,t) = U_0(x,y) + \varepsilon u_1(x,y,t) \\ v(x,y,t) = \varepsilon v_1(x,y,t) \\ p(x,y,t) = P_0 + \varepsilon p_1(x,y,t) \\ \rho(x,y,t) = \rho_0(x,y) + \varepsilon \rho_1(x,y,t) \end{cases} \tag{1}$$

The mean flow is supposed to be isentropic on each streamline. Then, introducing the set of equations (1) into the Euler equations and keeping the first order terms in ε leads to the Linearized Euler Equations (LEE). The mean flow's x-derivatives are simplified using the slowly varying flow assumption (WKB method) and the density is eliminated thanks to the hypothesis of barotropic pressure. Then we adopt the classical approach of stability writing the perturbations functions as normal modes with complex pulsation ω, wave number α and complex eigenfunctions depending on y only.

$$\begin{cases} u_1(x,y,t) = F(y)e^{i(\alpha x-\omega t)} \\ v_1(x,y,t) = G(y)e^{i(\alpha x-\omega t)} \\ p_1(x,y,t) = P(y)e^{i(\alpha x-\omega t)} \end{cases} \tag{2}$$

Then, the LEE equations read :

$$\begin{cases} i\rho_0 c_0^2 \alpha\, F + \rho_0 c_0^2\, \partial_y G + i(\alpha U_0 - \omega)P = 0 \\ i(\alpha U_0 - \omega)F + \partial_y U_0\, G + i\alpha\rho_0^{-1} P = 0 \\ i(\alpha U_0 - \omega)G + \rho_0^{-1}\partial_y P = 0 \end{cases} \tag{3}$$

where c_0 is the speed of sound in the mean flow.

Boundary conditions

On a wall, a slip condition will be imposed : $G = 0$. If no wall is present, we will match the solution with the analytic solution of the problem (3) for a uniform flow. In the following, this condition will be called the "Uniform Flow Solution Matching" (UFMS) condition.

Numerical resolution

The system (3) associated with the previous boundary conditions constitutes a generalized eigenvalue problem which is solved with a spectral collocation method based on the Chebyshev polynomials (M.R. Khorrami [7]). In the frame of a temporal study, α is fixed to a real value and the searched complex eigenvalue is ω. Then the generalized eigenvalue problem reads :

$$A^{\alpha}(U_0, \rho_0, c_0, \alpha)X = \omega B^{\alpha} X \tag{4}$$

In the case of a spatial study, ω is fixed to a real value, and the generalized eigenvalue problem reads :

$$A^{\omega}(U_0, \rho_0, c_0, \omega)X = \alpha B^{\omega} X \tag{5}$$

These problems are solved with standard LAPACK routines, for the resolution of generalized eigenvalue problems.

MEAN FLOW DEFINITION

In order to proceed to the stability analysis, a base flow is needed to give appropriate values to the coefficients U_0, ρ_0 and c_0 in the system (3).

Geometry and mean flow

The mean flow is extracted from a RANS calculation performed by S. Ben Khelil [2] around a 2D full wing with high lift devices, at 1/10th scale. The figure 2 shows a general view of the flow around the slat. In this case, the recirculation bubble behind the slat trailing edge is quite small (figure 3), approximatively as wide as the slat trailing edge width d.

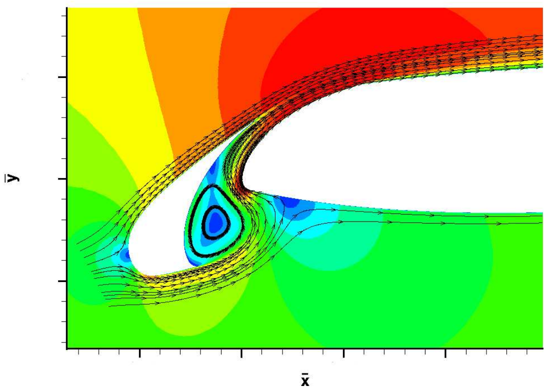

Figure 2: *General view of the slat flow*

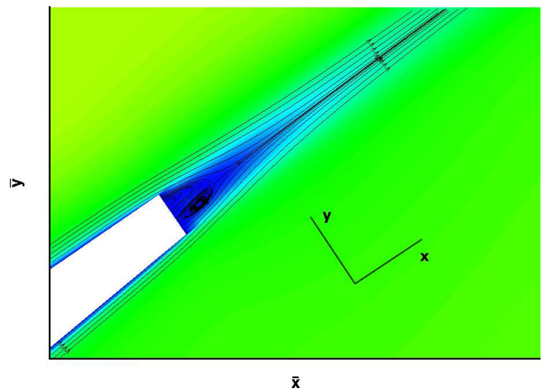

Figure 3: *Focus on the trailing edge flow*

Profiles extraction and interpolation

Extraction

The streamwise velocity u_l (figure 5) is made dimensionless by the speed of sound c_0, the streamwise and cross-tream coordinates (resp. ξ and η) by $d/2$. Three profiles for both the streamwise velocity and the density are extracted at different streamwise stations (cf. figure 4) : ξ_1 (the closest to the slat), ξ_2 and ξ_3 (the furthest). The first two profiles (ξ_1 and ξ_2) are in the recirculating zone, while the third one (ξ_3) is not. Furthermore, they are bounded by the main part of the wing for the lower boundary ($\eta = -52$), where a slip condition will be imposed ($G = 0$), and by the uniform flow field for the upper boundary ($\eta = 10$), where the UFSM condition will be applied.

Interpolation

There is no reason that the interpolation points and the collocation ones be the same, so an interpolation is needed to evaluate the profiles at the collocation points. We use a spline-based method that is easy to implement and economic in CPU time and memory. Furthermore, this method offers the ability to compute the first and second order derivatives of the fitted function.

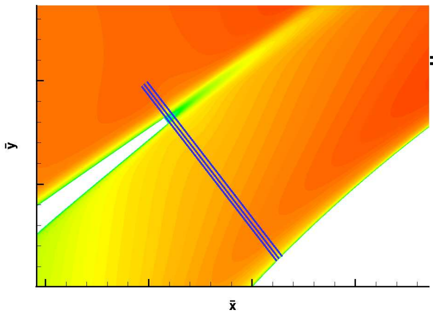

Figure 4: *Profile positions*

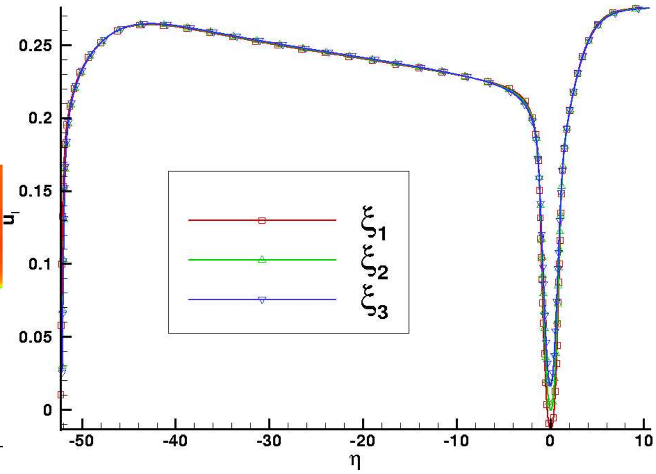

Figure 5: *Streamwise velocity*

STABILITY COMPUTATIONS

Now, all the coefficients of the system (3) are known thanks to the extraction and the interpolation of the RANS stationary mean field, so that the stability study can be performed.

Spatial study

For each profile, the generalized eigenvalue problem (5) is solved, with $\omega = 0.15$. A set of discrete values for α is obtained amongst which are artefacts of the collocation method. They are easily catchable as they move with the number of Chebyshev polynomials used, while the "physical modes" do not as soon as enough polynomials are used. There are four modes for the first profile, and two for the other two, at the considered pulsation. The spatial spectra are all symmetric with respect to the $Im(\alpha) = 0$ axis, which is typical of inviscid flow. After applying the Bers criterion [5] we find that only those with a negative imaginary part are amplified and that they propagate downstream.

Eigenvectors

The eigenvectors associated with the most amplified modes are computed. A normalization such that $\max_y(P(y)) = 1$ is done. The real and imaginary parts and the three eigenvectors F, G and P are shown in figures 6 and 7 for the amplified mode of the third profile, only for $\eta \in [-10, 10]$.

We can see that the cross-stream profiles are almost symmetric, while the pressure ones are almost antisymmetric. The same trend is observed on the other profiles. This is characteristic of a "sinuous" mode (Huerre & Rossi [6]), which according to the linear stability theory of symmetric wakes is the most amplified one. So this result seems to be applicable for our nearly symmetric wake.

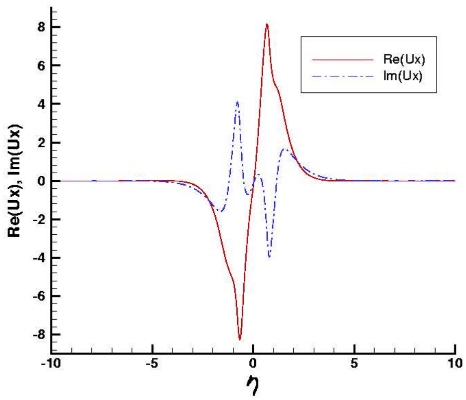

Figure 6: *Streamwise velocity*

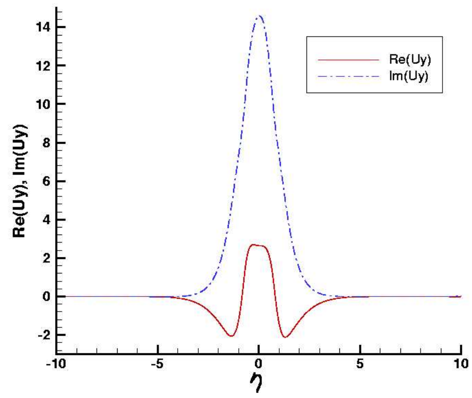

Figure 7: *Cross-tream velocity*

Absolute instabilities

An absolute instabilitie corresponds to a wave that spreads exponentially in the entire domain, and is characterized by the value of the pulsation of a stationary wavepacket in the $x/t = 0$ ray : the absolute pulsation which is denoted as ω_0. The real part of ω_0 will give us an approximate value of the vortex shedding freqency.

To find the value of ω_0, we apply the "Absolute Instability Criterion" (AIC) also named "Briggs criterion" [5]. According to it, the absolute instability is a saddle point of the dispersion relation in the plane (ω, α), associated with a cusp point in the (ω_r, α_r) and (ω_r, α_i) planes, and a coalescence of the spatial branches in the (α_r, α_i) plane.

So, by iterative resolution of the problems (4) and (5) we plot the curves $\omega_r \to \alpha_i(\omega_r, \omega_i)$, $\omega_r \to \alpha_r(\omega_r, \omega_i)$, and $\alpha_r \to \alpha_i(\omega_r, \omega_i)$, varying ω_i from 0 to a value that gives rise to a possible cusp point, with the coalescence of the spatial branches. If no cusp point is visible, nor coalescence, or if the value of the correponding ω_i is negative, no absolute instability occurs. In all other cases, the vortex shedding frequency is given (locally) by the dimensional absolute frequency :

$$f_0 = \frac{\omega_{0,r} c_0}{\pi d}.$$

As an illustration, we present in figure 8 and 9 the results for the first profile. In figures 8 we have a cusp point in $(\omega_r, \alpha_i) = (0.1175, -0.705)$, for $\omega_i = 0.023$. The coalescence of the spatial branches is visible in figure 9 for $\alpha = 1.082 - 0.705i$ and again $\omega_i = 0.023$. Here an absolute instability is characterized according to the AIC, as $\omega_{0,i} > 0$. We apply the AIC for the most amplified mode of the three profiles, and we find absolute instabilities only for the first two profiles.

The table 1 summarizes the values found. These frequencies are local, that is they do not necessarily correspond to the value of the global phenomenon, the vortex shedding. As the recirculation bubble is very small and the found values quite similar, we will keep a quantitative value around 40 kHz for the vortex shedding fequency. This value is in very good agreement with the tonal noise in the slat spectrum (figure 1). Computations have been made

Profile	ξ_1	ξ_2
ω_0	0,1175 + 0,023i	0,1212 + 0,013i
$f_0(Hz)$	38974	40217

Table 1: Absolute frequencies

on a 1/10 scale, so keeping constant the Strouhal number

$$St = \frac{f_0 d}{U_{ref}},$$

this gives rise to a frequency at a full-scale

$$f_0^\star = \frac{St U_{ref}}{d^\star} = 4kHz.$$

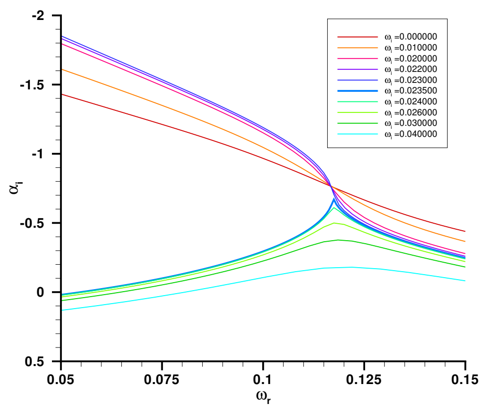

Figure 8: (ω_r, α_i) *plane*

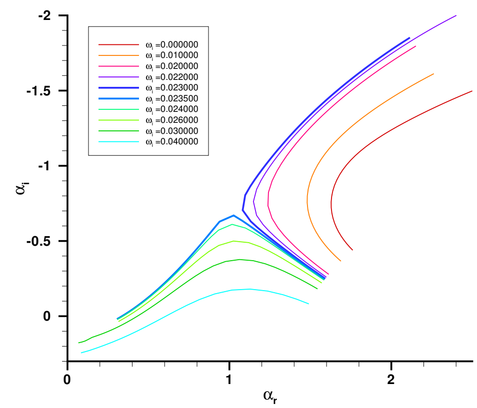

Figure 9: (α_r, α_i) *plane*

Boundary condition influence

Until now we have imposed a slip condition at the lower boundary of the domain ($\eta = -52$), and a UFSM condition at the upper boundary ($\eta = 10$). Now a stability analysis is performed on the truncated domain $[-10, 10]$, and a UFSM condition is imposed at both extremities.

We execute the same computations as above, and we find the same results. The direct conclusion is that is this case the main wing does not have any influence on the values of the absolute instabilities. This is easy to understand when looking at the eigenvectors (figures 6 and 7). They are damped very early (for $\eta < -5$ and $\eta > 5$) in comparison with the distance to the main part of the wing ($\eta = -52$).

CONCLUSIONS

Thanks to linear stability tools, a quantitative value of the vortex shedding frequency has been computed at very low computing cost. The value found, for the 1/10 scale, near 40 kHz is in good agreement with existing measurements and computations that, for different experimental or computational conditions, give results from 30 kHz to 50 kHz for the same scale.

Moreover, the present study has been able to confirm the existence of a pocket of absolute instability, which seems to correspond roughly with the recirculation bubble. This pocket acts as a hydrodynamic oscillator and creates the vortex shedding.

We have also shown that there is no influence of the main part of the wing on the vortex shedding frequency.

REFERENCES

References

[1] M.R. Khorrami, M. Choudhari, B.A. Singer, D.P. Lockard and C.L. Street, “In search of the physics: the interplay of experiment and computation in slat aeroacoustics”, AIAA Paper 2003-0980 (2003).

[2] S. Ben Khelil, C. François, F. Moens and I. Mary, “Calcul d’écoulements autour d’un profil NACA0012 à bord de fuite tronqué et d’un profil hypersustenté en vue de la prévision numérique du bruit rayonné”, ONERA, RT 10/05628/DSNA/DAAP (November 1990).

[3] M.R Khorrami, M.N. Choudhari and L.N. Jenkins, ”Characterization of Unsteady Flow Structures Near Leading-Edge Slat : Part II. 2D Computations”, NASA, AIAA Paper 2004-2802 (2004)

[4] W. Dobrzynski and M. Pott-Pollenske, ”Slat noise source studies for farfield noise prediction”, DLR, AIAA Paper 2001-2158 (2001)

[5] A. Bers, “Space-time evolution of plasma instabilities - absolute and convective”, Handbook of Plasma Physics - Volume 1 : Basic Plasma Physics, pp. 451-517, North-Holland Publishing Company (1983)

[6] P. Huerre and M. Rossi, “Hydrodynamic instabilities in open flows”, Hydrodynamics and nonlinear instabilities, pp 81-198, Cambridge University Press (1998)

[7] M.R. Khorrami, M.R. Malik and R.L. Ash, “Application of Spectral Collocation Techniques to the Stability of Swirling Flows”, Journal of Computational Physics, **81**, pp 206-229 (1989)